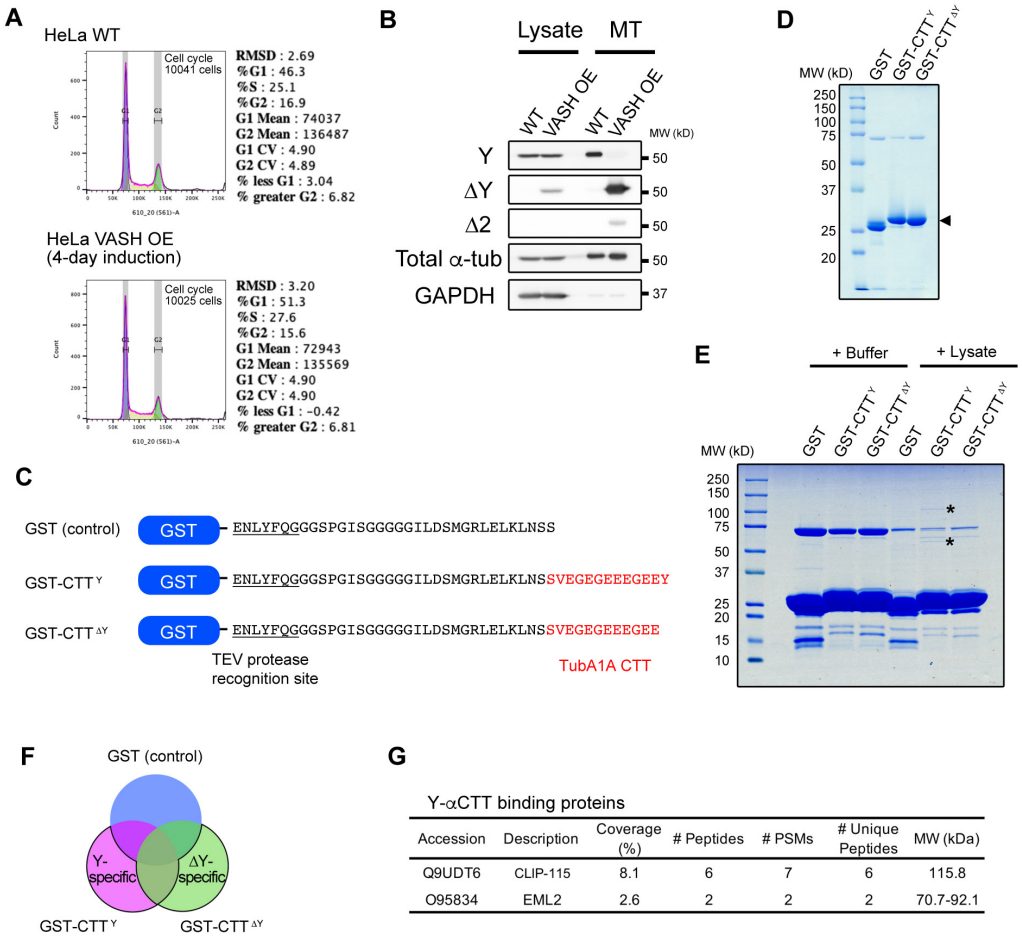

Accession	Description	Coverage (%)	# Peptides	# PSMs	# Unique Peptides	MW (kDa)
Q9UDT6	CLIP-115	8.1	6	7	6	115.8
O95834	EML2	2.6	2	2	2	70.7-92.1

Figure S1. Identification of proteins preferentially interact with Y- and ΔY-αCTTs, related to Figure 1.

(A) Cell cycle analysis for HeLa WT and VASH OE cell lines. WT HeLa cells and VASH OE cells cultured in the presence of doxycycline for 4 days were stained with propidium iodide and analyzed with flow cytometry. There is no significant difference between the parental and VASH1 over-expressing HeLa cells.

(B) Comparison of the levels of α-tubulin detyrosination in HeLa WT and VASH1/SVBP overexpressing cell lines. Immunoblot analysis for tubulin Y/ΔY state in lysates (Lysate) and microtubule pellet fractions (MT) prepared from WT HeLa and HeLa cells overexpressing VASH1-SVBP (VASH OE). After the Taxol-induced microtubule assembly, Y-tubulin decreased to an undetectable level in the VASH1 OE conditions.

(C) GST-CTT constructs used for the pulldown experiment for identification of CTT binding proteins.

(D) Purified GST and GST-CTT proteins analyzed on a gel. An arrowhead indicates the position of GST and GST-CTT proteins. Higher molecular weight bands are likely GST dimers.

(E) Proteins pulled down with GST, GST-CTT^{Y} and GST-CTT$^{\Delta Y}$ in buffer (control) or CHL-1 cell lysates were analyzed on a gradient gel. Asterisks indicate proteins detected specifically in the GST-CTT^{Y} pulldown.

(F) Venn diagram of MS analysis. CTT binding proteins were defined as proteins detected in GST-CTT (Y/ΔY) pulldown but are absent in the control GST pulldown. Among them, GST-CTT^{Y}- and GST-CTT$^{\Delta Y}$-specific proteins were candidates of Y-CTT and ΔY-CTT-readers, respectively.

(G) Y-αCTT binding proteins identified by LC-MS/MS. MAPs that were identified with minimum 2 unique peptides are shown in the table. Also see Data S1.

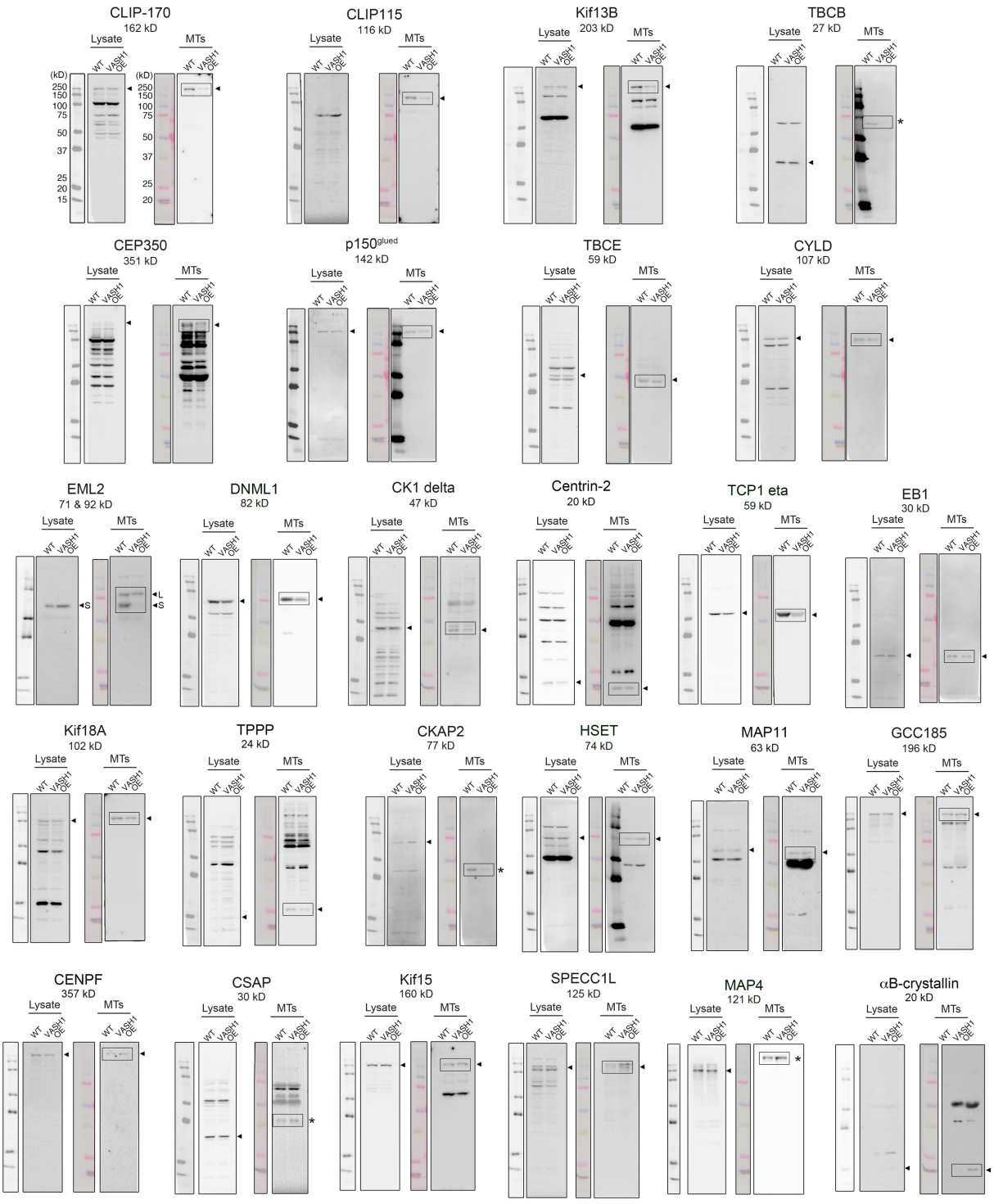

Figure S2. Immunoblot analysis of proteins identified with the TMT screening in whole cell lysates and microtubule pellet fractions, related to Figure 1.

For each protein, blots for lysate (Lysate; left) and microtubule pellet fractions (MTs; right) are shown. Boxed areas were cropped and shown in Figures 1E and 1F. Expected molecular weight and band positions, based on the canonical sequence reported on Uniport, are indicated under the protein name and by arrowheads. The positions of bands denoted with asterisks are inconsistent with their predicted molecular weights.

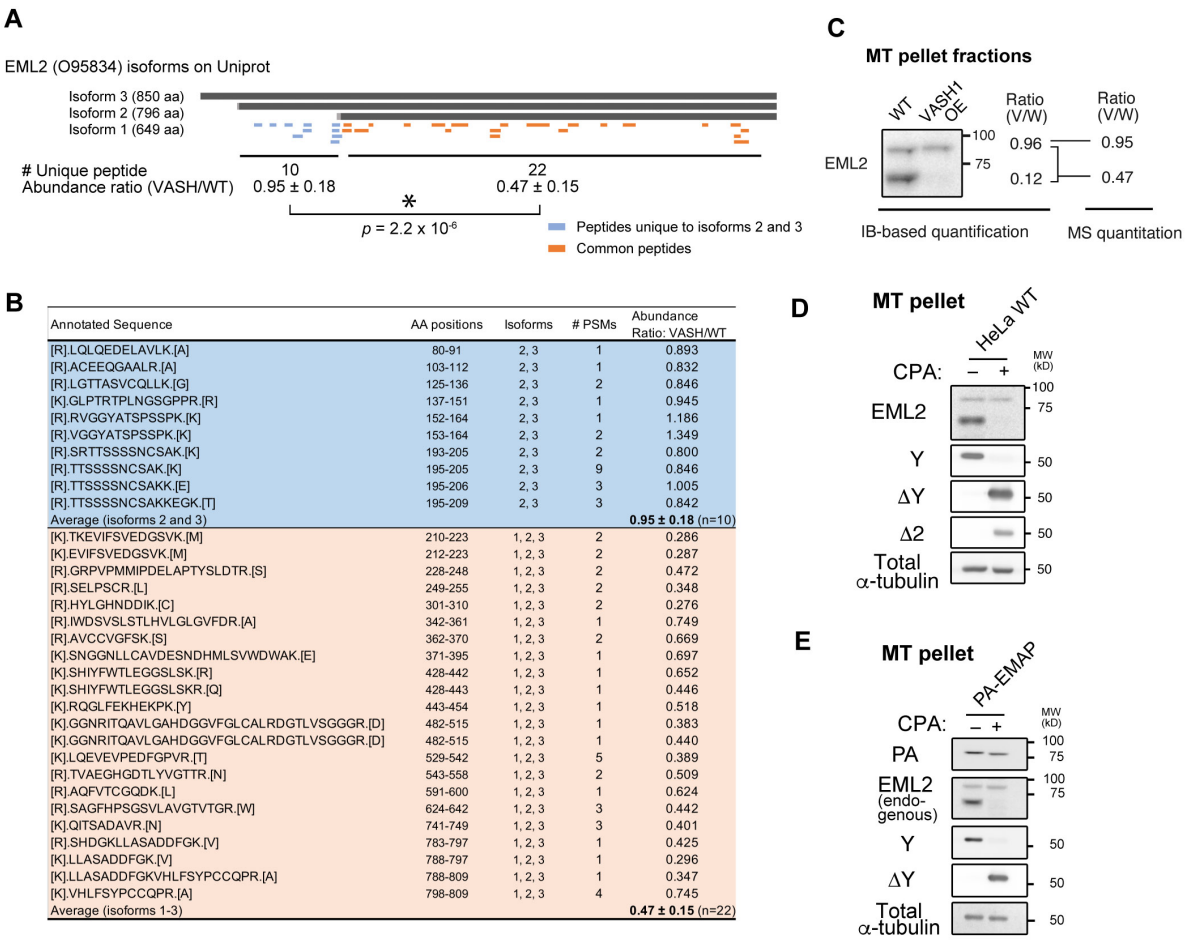

Figure S3. Detection of EML2 isoforms in fractions co-sedimented with Y- and ΔY-microtubules, related to Figure 2.

(**A**) EML2 peptides identified in the MS analysis. Peptides derived from longer isoforms (2 and 3) are depicted with blue bars whereas peptides that are common to any isoforms are shown in orange. Relative abundance of these peptides [see (C)] are averaged and shown.

(**B**) List of EML2 peptides identified in the TMT analysis. The same color code was used as (A).

(**C**) Comparison between immunoblot (IB)- and MS-based quantification of relative abundance of EML2 isoforms. Densitometric analysis was normalized against corresponding total α-tubulin blot.

(D) Alternative method of Y/ΔY microtubule preparations using carboxypeptidase A (CPA)-mediated α-tubulin detyrosination in HeLa WT lysate. HeLa lysate was treated with CPA prior to the microtubule assembly. Microtubule pellet fractions in untreated (–) or CPA-treated (+) lysates were analyzed with immunoblot. Although a small fraction of Δ2 tubulin was generated, Y/ΔY binary conditions were comparable to the WT/VASH1 OE method. EML2-S was absent in the microtubule pellet prepared from CPA-treated lysate.

(E) Microtubule co-sedimentation assay for PA-tagged sea urchin EMAP overexpressed in HeLa cells. PA-EMAP was detected at similar levels in both Y- and ΔY-microtubule pellet fractions generated with CPA. EML2 blot was shown as a positive control.

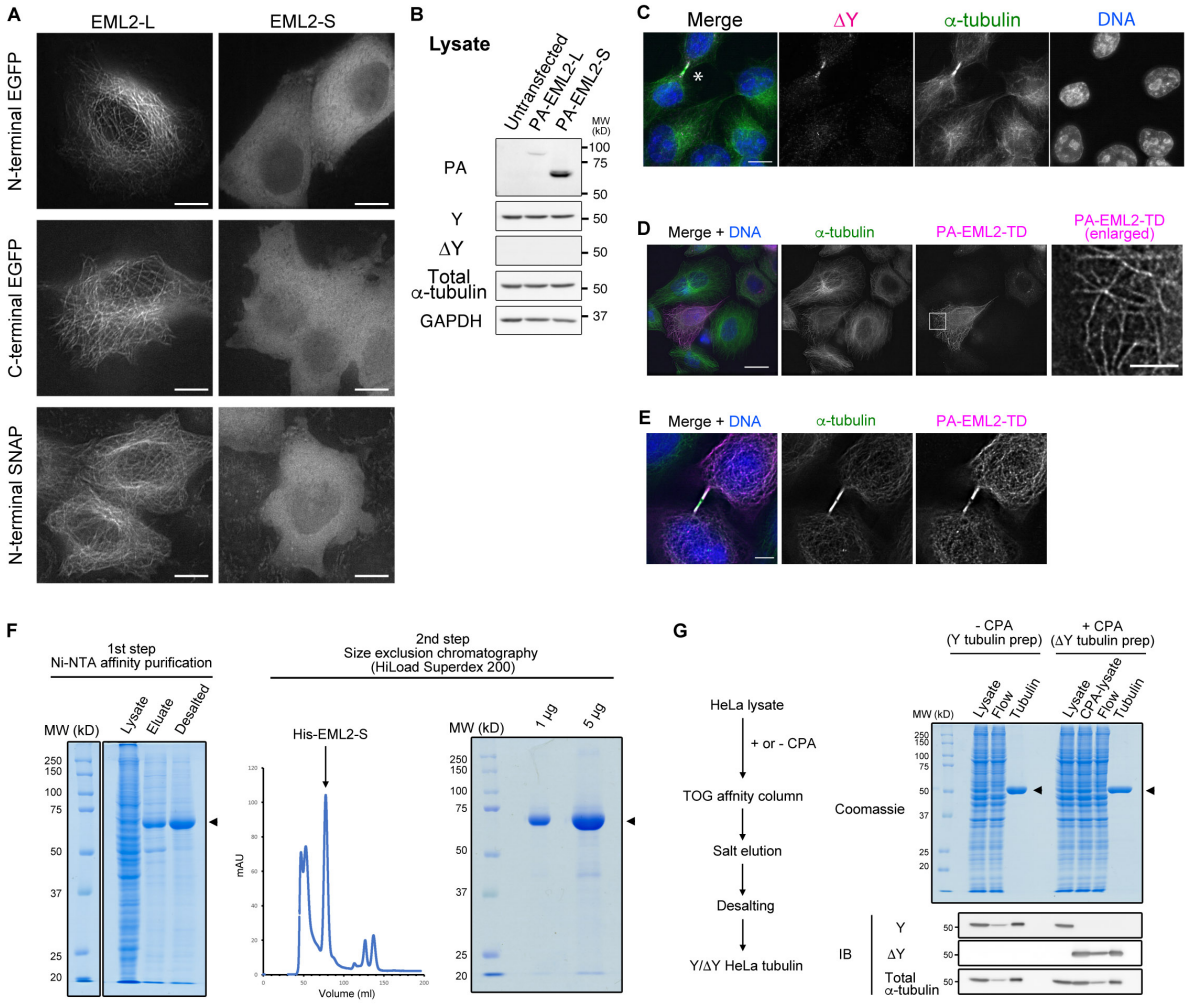

Figure S4. Y-αCTT preference of EML2-S examined with cell-based and *in vitro* assays, related to Figure 3.

(A) Live imaging of HeLa cells transiently expressing EGFP (N-/C-terminal) or SNAP-tagged EML2-L/S. HeLa cells were transfected with corresponding constructs and imaged. EML2-S did not exhibit microtubule localization when fused to bulky tags. Scale bars, 10 μm.

(B) Immunoblot analysis for lysates prepared from HeLa cells transiently expressing PA-EML2-L or S. Lysates were prepared from HeLa cells transfected with PA-EML2 constructs and analyzed. A total of 15 μg of proteins was loaded in each lane. PA-EML2 overexpression did not alter the Y/ΔY state in cells.

(C) Immunofluorescent staining of ΔY-microtubules in HeLa cells. ΔY signals were enriched in microtubules in the midbody (asterisk). Scale bar, 10 μm.

(D and E) Immunofluorescent staining of PA-EML2-L TD overexpressed in interphase HeLa cells **(D)** and cells undergoing cytokinesis **(E)**. Scale bars, 20 μm (D) and 5 μm (E).

(F) Purification of His-EML2-S from insect cells. His-EML2-S was purified by two steps: Ni-NTA affinity chromatography (left) followed by size exclusion chromatography (right). Arrowheads indicate the position of His-EML2-S on SDS-PAGE gels. A representative elution profile is shown in the middle with an arrow indicating the peak fractions corresponding to His-EML2-S.

(G) Purification of Y- and ΔY-tubulin from HeLa cells using TOG affinity chromatography. A workflow (left) and images of a gel and blots for representative preps (right) are shown. Prior to the affinity purification step, HeLa lysates were treated with or without CPA for ΔY or Y-tubulin preps, respectively. Arrowheads indicate the positions of Y- and ΔY-tubulin.

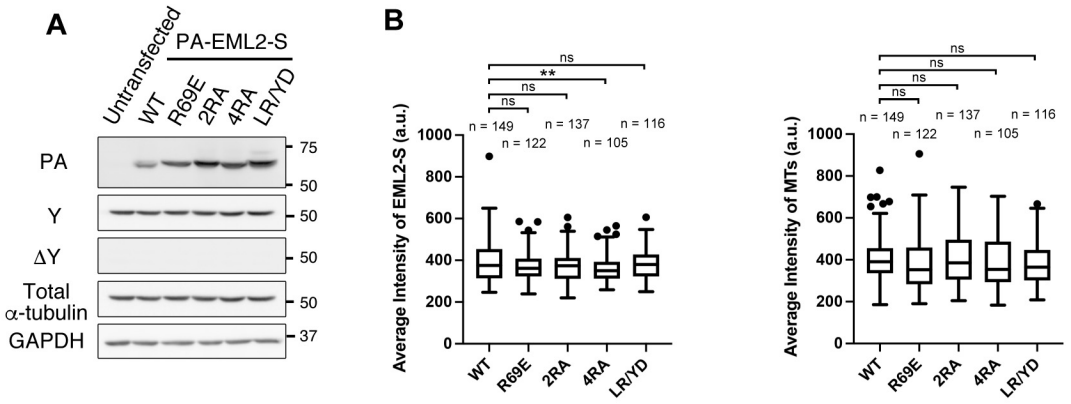

Figure S5. Transient expression of PA-EML2-S mutants in HeLa cells, related to Figure 4.
(A) Immunoblot analysis of lysates prepared from HeLa cells transiently expressing PA-EML2-S mutants. A total of 15 μg of proteins was loaded in each lane. Comparable levels of PA-EML2-S proteins were detected. The Y/ΔY state was not affected by overexpression of PA-EML2 mutants.
(B) Quantification of average intensities of EML2-S mutants and microtubules (MTs) in the immunostained HeLa cells. Fluorescent intensities of PA-EML2-S mutant proteins as well as microtubules were comparable among different constructs. The box and line indicate 75th and 25th percentile, and median, respectively. Whiskers and outliers (shown by dots) are plotted by the Tukey method. **, $p < 0.05$; ns, no significance.

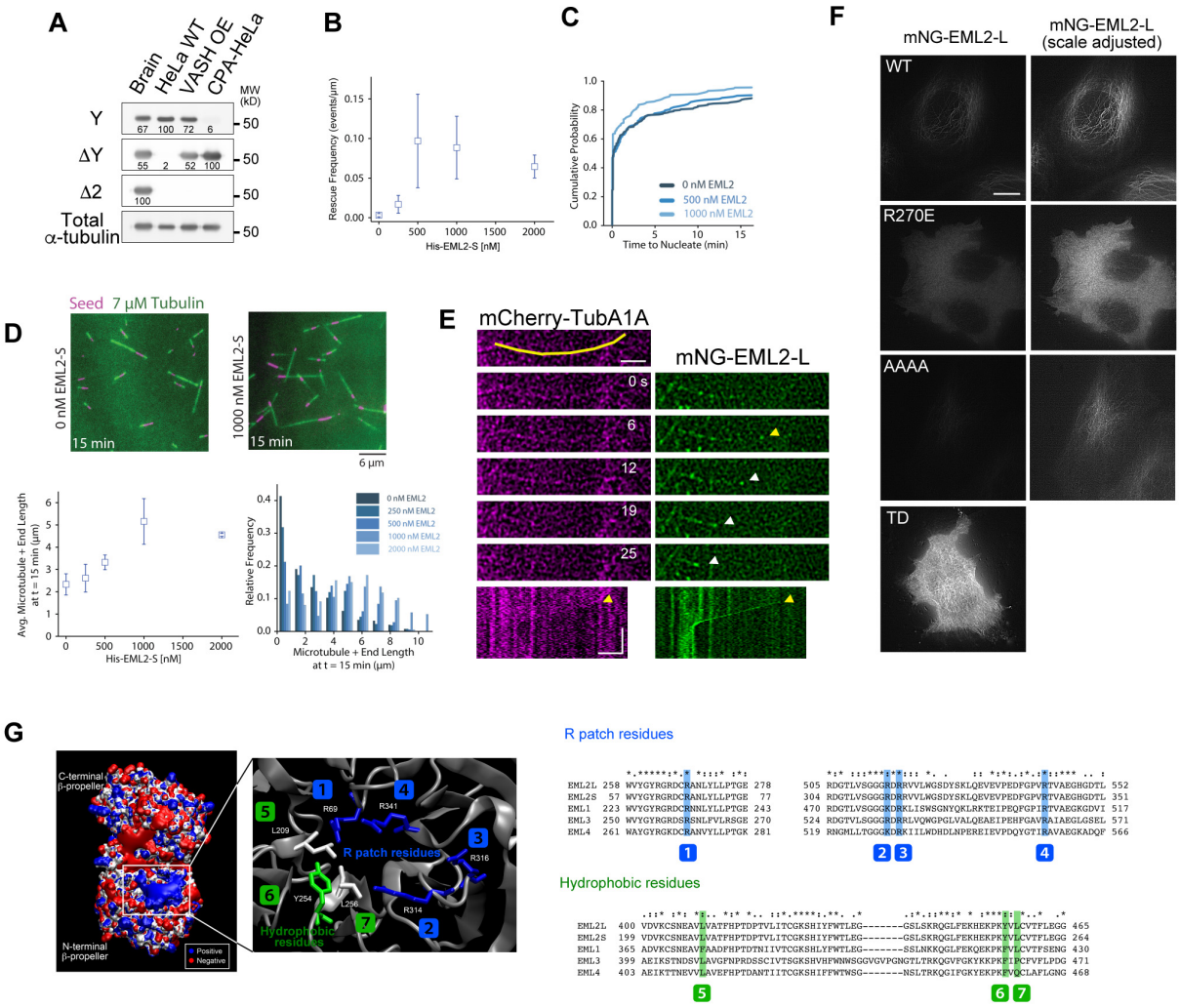

Figure S6. Functional analysis of EML2-L and S using live cell imaging and *in vitro* microtubule dynamics assay, related to Figures 5 and 6.

(A) Comparison of Y/ΔY/Δ2 levels in different tubulin samples used in this study. Bovine brain tubulin (Brain), HeLa tubulin without CPA treatment (HeLa WT), tubulin purified from VASH OE HeLa cells (VASH OE) and HeLa tubulin purified from WT HeLa lysate treated with CPA (CPA-HeLa) are shown. Band intensities were measured, normalized against total α-tubulin and shown at the bottom of each blot (% of max).

(B-D) Additional microtubule dynamics parameters measured in the *in vitro* assay using purified His-EML2-S protein. Alternate rescue frequency described in number of events per microtubule length (events/μm) **(B)**. Cumulative probability of microtubule nucleation **(C)**. His-EML2-S shows minimum impact on the microtubule nucleation. Representative TIRF images of microtubules at 15 min and measurements of microtubule length **(D)**. Magenta, seeds; green, elongated microtubules. Scale bar, 6 μm.

(E) Time lapse imaging of a microtubule in a HeLa cell co-expressing mCherry-TubA1A and mNG-EML2-L. Arrowheads mark the position of shortening microtubule ends. Yellow arrowheads indicate the beginning of a microtubule shortening event. Vertical bar, 30 s; horizontal bars, 2 μm.

(F) Transient expression of mNG-EML2-L mutants in HeLa cells. Scale bar, 10 μm.

(G) Sequence alignments of EML1-4 TAPE domains. Conserved residues in the R-patch (blue) and the hydrophobic clamp (green/white) were mapped in the ribbon diagram (left) and indicated in the aligned sequence (right). Multiple sequence alignment was performed using ClustalX 2.1 (http://www.clustal.org/clustal2/).